Appendix 1

Here we compare the proposed CLOSE3D method with relatively new, previously existing algorithms, including the quality-guide and graph-cut phase-unwrapping algorithms. One simulated Gaussian phase cube (256×256×100) was generated to compare CLOSE3D with relatively new, previously existing algorithms, including the region-growing (RG) (22), Graph_cut (31), and SEGUE (32) phase-unwrapping algorithms. The original phase was calculated as:

$$\phi_{x,y,z} = 25 \times (1 + 0.1 \times z) \times e^{-\frac{x^2+y^2}{2}} \quad [S1]$$

where x, y, and z are spatial positions, and the SD was 40 pixels. The magnitude increased from 10 to 120 in increments of 10 in the xOy plane. Gaussian noise with SD of 20 rad was added. The MCR was calculated as the incorrect unwrapped pixel ratio in VOI. The simulation was repeated 20 times, and the corresponding means and SDs of error ratio (%), and running time(s) were separately calculated.

Figure S1 shows the phase-unwrapping results by RG, Graph_cut, SEGUE, and CLOSE3D under different noise levels in a clockwise direction in the xOy plane, and different phase variation levels along the z axis direction. There are obvious wraps in the results by the RG, Graph_cut, and SEGUE methods, whereas the proposed method obtained a smooth unwrapped phase. The means and SDs of the error ratios by RG, Graph_cut, and SEGUE were 39.25%±15.88%, 4.18%±0.07%, and 13.19%±0.69%, respectively, which were all larger than that with CLOSE3D. The mean and SD of the error ratio with the proposed method was 0.14%±0.01%. The means and SDs of the running time with RG, Graph_cut, SEGUE and the proposed method were 4.8±0.1 s, 9,769.8±813.3 s, and 13,349.9±1,173.3 s and 18,150.5±1,526.6 s, respectively. The RG and Graph_cut methods were faster than the SEGUE and CLOSE3D algorithms. Graph_cut and RG were programed by C, whereas SEGUE and the proposed method were programed by MATLAB. After running more than 24 h, the unwrapped phase by the PRELUDE method had not been generated.

To show the accuracy in the regions with the discontinued phase, one simulated Gaussian phase cube (128×128×64) was generated; the original phase was calculated as:

$$\phi_{x,y,z} = 30e^{-\frac{x^2+y^2+z^2}{2}} \quad [S2]$$

where x, y, and z are spatial positions, the SD was 25 pixels and the magnitude was 100. Gaussian noise with SD of 10 rad was added. The pixels in the predefined ring region were set to zero.

Figure S2 shows the phase-unwrapping results of the simulated data with disconnected phase regions by RG, Graph_cut, SEGUE, and CLOSE3D. There are obvious wraps in the results of the RG, Graph_cut, and SEGUE methods, whereas the CLOSE3D obtains a smooth unwrapped phase.

The independent sample Student's *t*-test was used to illustrate the performance difference of the 3 methods by rigorous statistical comparison of the results of the simulated dataset with different noise levels. The statistical comparisons of the error ratios of RG and PRELUDE with that of the CLOSE3D over the simulated data with different noise levels are shown in *Table S1*. When the noise level was <40%, the means and SDs of the error ratio by the 3 methods were all 0.00%±0.00%. The independent sample Student's *t*-test could be not used, which indicates that there is no difference between RG and CLOSE3D, and PRELUDE and CLOSE3D. When the noise level was equal to 40%, the means and SDs of the error ratio by the 3 methods were 0.90%±0.16%, 0.01%±0.01% and 0.01%±0.01%, respectively. The independent sample Student's t-test results indicated that the error ratio of RG (P=0.001) was significantly higher than that of CLOSE3D. When the noise level was equal to 60%, the means and SDs of the error ratio by the 3 methods were 32.00%±23.56%, 0.20%±0.17% and 0.08%±0.09%, respectively. The independent sample Student's *t*-test results indicated that the error ratios of RG (P=0.000) and PRELUDE (P=0.007) were significantly higher than that of the proposed method. When the noise level was equal to 80%, the means and SDs of the error ratio by the 3 methods were 47.14%±37.38%, 0.65%±0.63% and 0.22%±0.23%, respectively. The independent sample Student's *t*-test results indicated that the error ratios of RG (P=0.000) and PRELUDE (P=0.014) were significantly higher than that of the proposed method.

The quantitative analysis of QSM values in deep grey matter nuclei is shown in *Figure 5*. We present 2 representative axial slices of QSM from volunteers in *Figure S3*. The subcortical structures of the targeted deep grey matter nuclei were directly identified and manually segmented on the QSM images using the ITK-SNAP software (33). The means and SDs of the QSM

https://dx.doi.org/10.21037/qims-22-525

values of the subcortical structures are reported in *Table S2*. The variations in QSM values for the subcortical structures are essentially consistent with the reference (34).

We used simulated data to compare the error ratios and running times for CLOSE3D using 2-order and 3-order polynomial functions. One simulated Gaussian phase cube (128×128×64) was generated; the original phase was calculated as follows:

$$\phi_{x,y,z} = 30e^{-\frac{x^2+y^2+z^2}{2}} \quad [S3]$$

Where x, y, and z are spatial positions, the SD was 25 pixels and the magnitude was 100. Gaussian noise with SD of 50 rad was added. The simulation was repeated 20 times, and the corresponding means and SDs of the error ratio (%), and running time(s) were separately calculated.

Figure S4 shows the 3D unwrapped results for the simulated data with CLOSE3D using 2-order and 3-order polynomial functions. There are very few error voxels in the unwrapped results. The mean and SD of the error ratio by CLOSE3D using 2-order polynomial function was 0.01%±0.01%, which is slightly larger than that of CLOSE3D using 3-order polynomial function. The mean and SD of the error ratio by CLOSE3D using 3-order polynomial function was 0.003%±0.003%. The mean and SD of running time by CLOSE3D using 2-order polynomial function was 2019.2±179.7 s. However, the mean and SD of running time by CLOSE3D using 3-order polynomial function is 3519.2±332.7 s, which is much slower.

References

31. Dong J, Chen F, Zhou D, Liu T, Yu Z, Wang Y. Phase unwrapping with graph cuts optimization and dual decomposition acceleration for 3D high-resolution MRI data. Magn Reson Med 2017;77:1353-8.
32. Karsa A, Shmueli K. SEGUE: A Speedy rEgion-Growing Algorithm for Unwrapping Estimated Phase. IEEE Trans Med Imaging 2019;38:1347-57.
33. Yushkevich PA, Piven J, Hazlett HC, Smith RG, Ho S, Gee JC, Gerig G. User-guided 3D active contour segmentation of anatomical structures: significantly improved efficiency and reliability. Neuroimage 2006;31:1116-28.
34. Xu M, Guo Y, Cheng J, Xue K, Yang M, Song X, Feng Y, Cheng J. Brain iron assessment in patients with First-episode schizophrenia using quantitative susceptibility mapping. Neuroimage Clin 2021;31:102736.

https://dx.doi.org/10.21037/qims-22-525

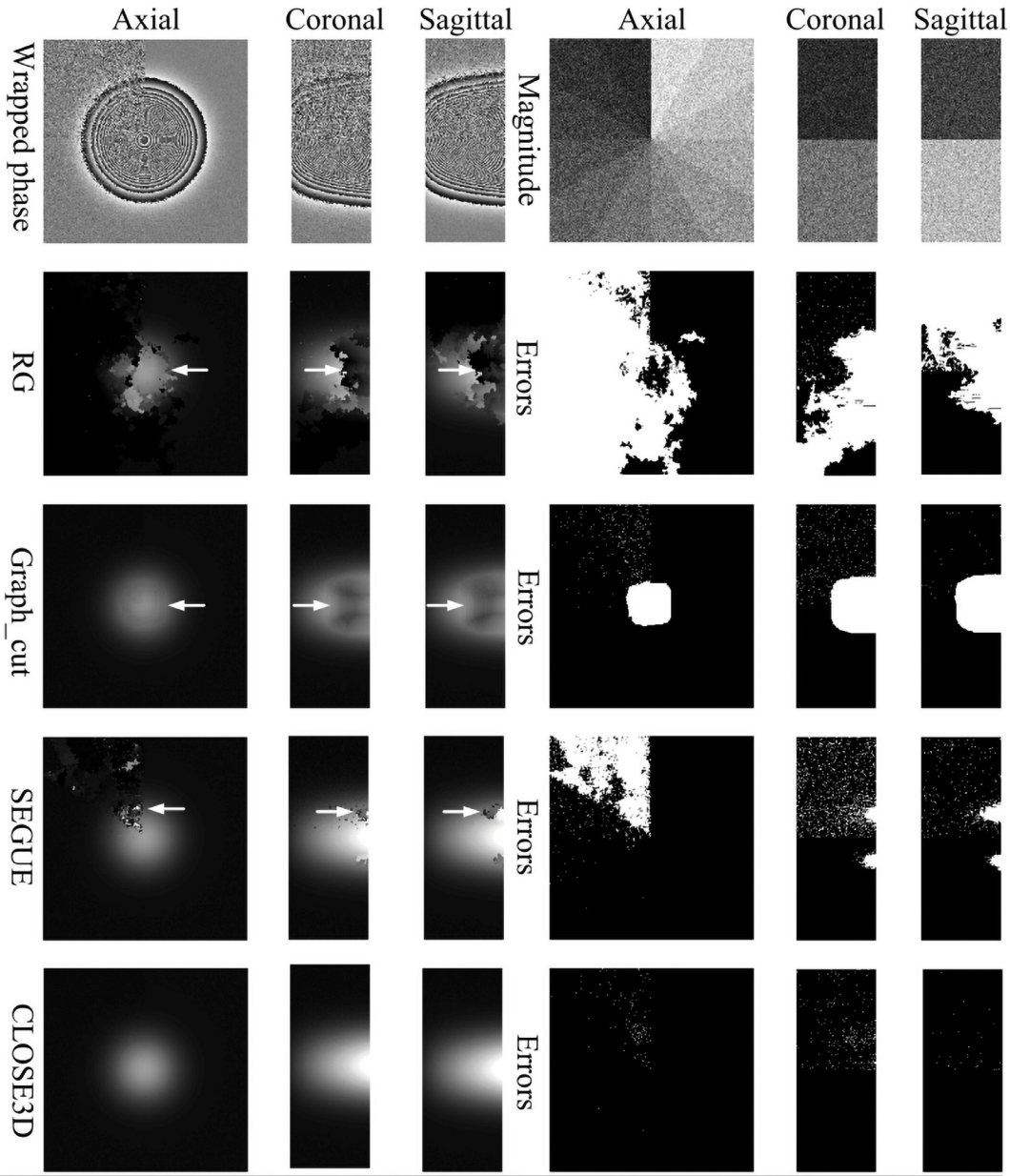

Data	Method	Error ratio (Mean ± SD, %)	Running time (Mean ± SD, s)	Language
Simulation 256×256×100	RG	39.25 ± 15.88	4.8 ± 0.1	C
	Graph_cut	4.18 ± 0.07	9769.8 ± 813.3	C
	SEGUE	13.19 ± 0.69	13349.9 ± 1173.3	Matlab
	CLOSE3D	0.14 ± 0.01	18150.5 ± 1526.6	Matlab

Figure S1 Unwrapped results of the simulated Gaussian phase cube with different SNRs in the clockwise direction in the xOy plane, and different phase variation levels along the *z* axis by the RG, Graph_cut, SEGUE, and CLOSE3D methods. Arrows indicate obvious error residues. The means and SDs of the MCR, running time, and programming language are shown.

https://dx.doi.org/10.21037/qims-22-525

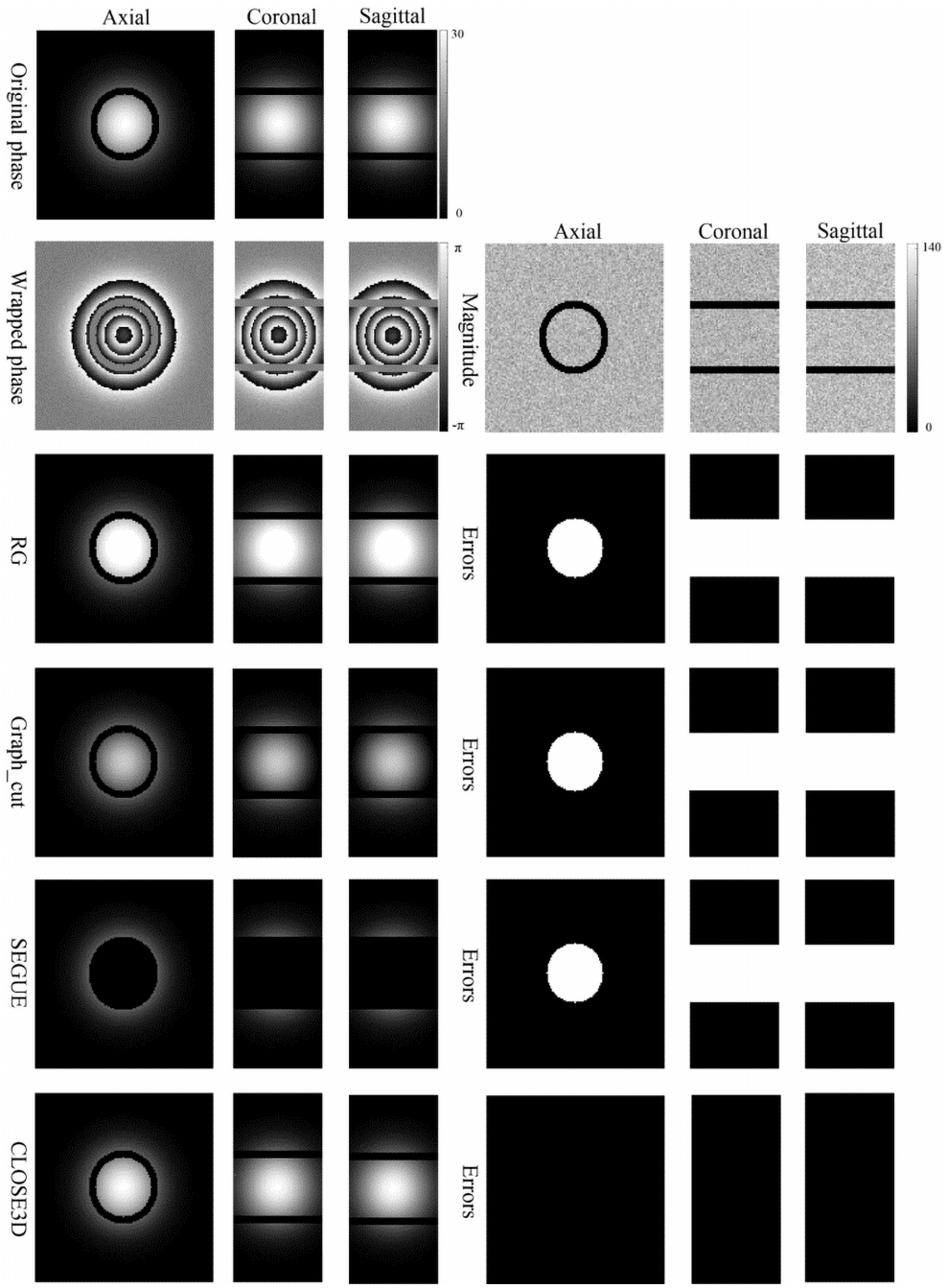

Figure S2 3D unwrapped results of the simulated data with disconnected phase regions by the RG, Graph_cut, SEGUE, and CLOSE3D methods. The original phase is the summation of added noise and true phase generated by Eq. S2.

https://dx.doi.org/10.21037/qims-22-525

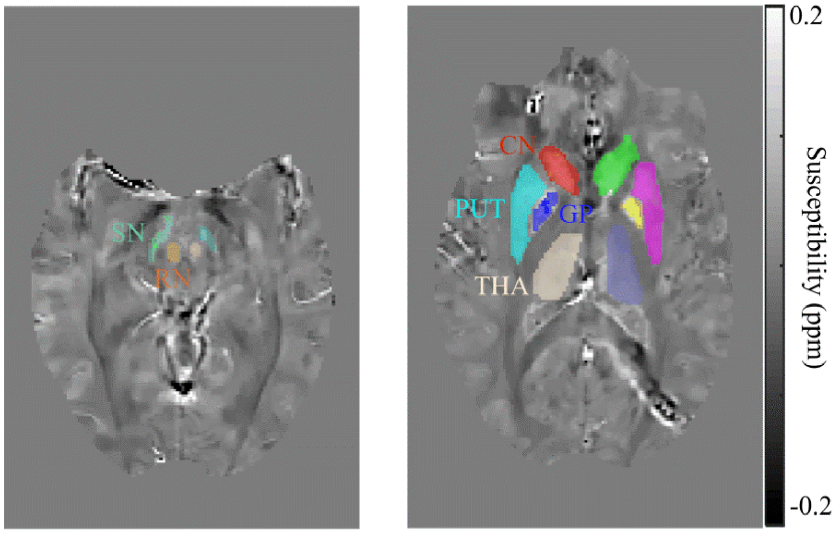

Figure S3 Two representative axial slices of QSM images from the cerebral hemorrhage volunteers with color overlay of targeted deep grey matter nuclei. QSM, quantitative susceptibility mapping; SN, substantia nigra; RN, red nucleus; CN, caudate nucleus; PUT, putamen; GP, globus pallidus; THA, thalamus.

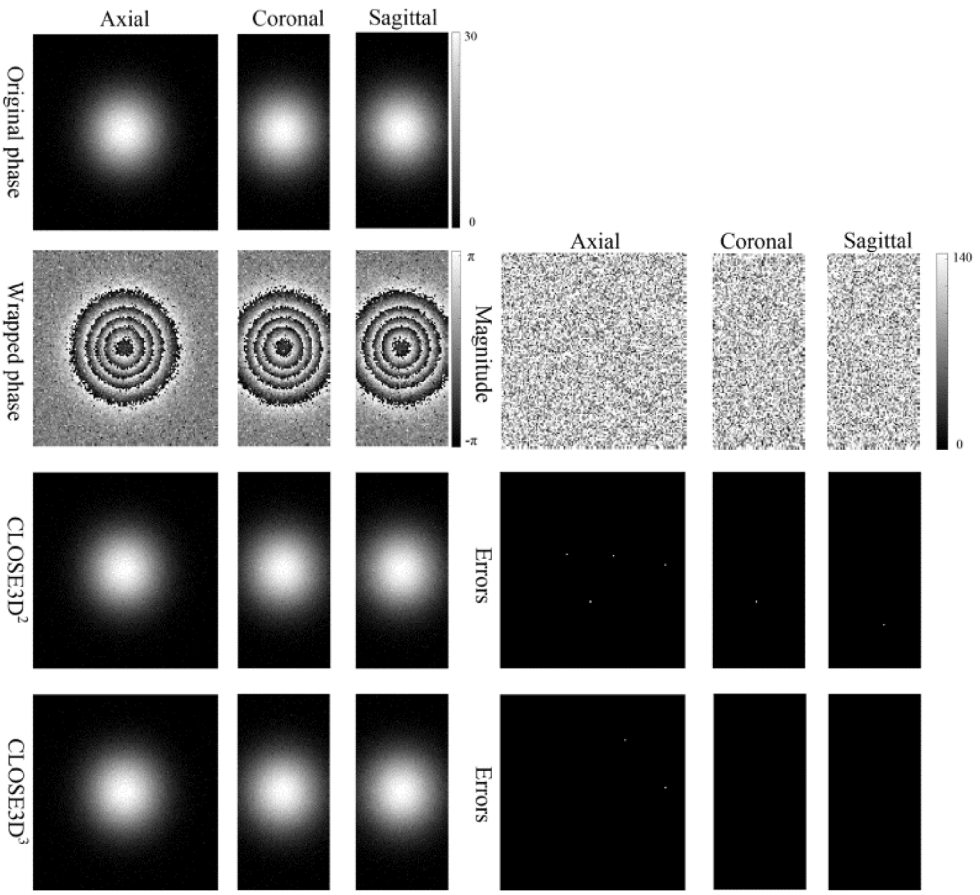

Figure S4 3D unwrapped results for the simulated data by CLOSE3D using 2-order and 3-order polynomial functions. The original phase is the summation of added noise and true phase generated by Eq. S3. The results in the second and third rows were separately unwrapped by CLOSE3D using 2-order and 3-order polynomial functions.

https://dx.doi.org/10.21037/qims-22-525

Table S1 Statistical comparison of the error ratios of RG and PRELUDE with that of CLOSE3D over the simulated data with different noise levels

Simulated data	Method	Error ratio (Mean ± SD, %)	P value
0% noise	RG	0.00±0.00	N/A
	PRELUDE	0.00±0.00	N/A
	CLOSE3D	0.00±0.00	N/A
20% noise	RG	0.00±0.00	N/A
	PRELUDE	0.00±0.00	N/A
	CLOSE3D	0.00±0.00	N/A
40% noise	RG	0.90±0.16	0.001
	PRELUDE	0.01±0.01	0.193
	CLOSE3D	0.01±0.01	N/A
60% noise	RG	32.00±23.56	0.000
	PRELUDE	0.20±0.17	0.007
	CLOSE3D	0.08±0.09	N/A
80% noise	RG	47.14±37.38	0.000
	PRELUDE	0.65±0.63	0.014
	CLOSE3D	0.22±0.23	N/A

Table S2 Regional QSM values for the cerebral hemorrhage volunteers (mean ± SD, ppm)

Data	Location	SN	RN	CN	PUT	THA	GP
Three volunteers	Left	0.119±0.027	0.059±0.020	0.046±0.022	0.033±0.024	0.012±0.010	0.127±0.031
	Right	0.107±0.024	0.062±0.019	0.039±0.021	0.038±0.024	0.012±0.011	0.126±0.026

QSM, quantitative susceptibility mapping; SN, substantia nigra; RN, red nucleus; CN, caudate nucleus; PUT, putamen; THA, thalamus; GP, globus pallidus; SD, standard deviation

https://dx.doi.org/10.21037/qims-22-525